

River Dune Behaviour in Dredged Areas

W.S. Kruis¹, L.R. Lokin^{1,2}, R.P. Van Denderen², S.J.M.H. Hulscher¹

¹Department of Civil Engineering, University of Twente, Enschede, The Netherlands

²HKV, Lelystad, The Netherlands

Key Points:

- Post-dredging river dune behaviour
- Two dimensional continuous wavelet analysis
- Influence of different dredging strategies on dunes

Corresponding author: L.R. Lokin, l.r.lokin@utwente.nl

Abstract

Ensuring safe navigation in rivers usually requires repeated dredging operations. River dunes are a significant source of shallow areas, so a better understanding of their behaviour can aid decision-making on dredging strategies. A new 2D wavelet tool was used to track and analyse dunes in this study. Alongside the dredging data from the river Waal, the investigation examined how the dunes behaved after dredging, and assessed the impact of topping (removing sediment from the crest) and swiping (transferring sediment from the crest to the trough) dredging methods. According to the results, it appears that dunes subjected to dredging recover gradually over time, exhibiting slow development. Higher growth rates result from higher dredging intensities. At the beginning stages, the growth of dredged dunes shows less variation in comparison to the unaffected ones, indicating that such dunes are less prone to flow conditions and other fluvial processes. For the dredging intensities performed in this study, topping has a more pronounced effect on the immediate reduction of dune height than swiping. Over the long term, topped dunes exhibit larger growth rates than those undergoing swiping, while the latter method is less disruptive to the sediment balance.

1 Introduction

Dredging is a regular activity in many rivers to maintain the minimum depth necessary for navigation (Knaapen & Hulscher, 2002). Maintenance dredging is used to deepen local shallow areas. The shallowest points typically arise from a shoal resulting from large-scale morphological features, such as river bends or side channels, combined with the presence of river dunes. Droughts triggered by climate change (Mukherjee et al., 2018) are causing rivers to experience a decline in water levels. As a result, the challenge of maintaining the minimum navigable depths in rivers is becoming more difficult, leading to an increase in the need for dredging. Enhancing our understanding of dune behaviour can aid in decision-making when establishing a maintenance strategy and reducing associated expenses. Thus, understanding the impact of dredging on river dune behaviour is vital for the improvement of future river management.

River dunes are rhythmic features that exist on the bed of river channels. Dunes are found in all major rivers of the world. They play a crucial role in transporting bed load sediment and significantly contribute to the roughness of the bed as well as the obstruction of the flow (Cisneros et al., 2020). River dunes propagate downstream due to erosion on the stoss side and sediment deposition on the lee side (Naqshband et al., 2021). River dunes are dynamic bed forms that adapt to changing flow and sediment transport conditions (Allen, 1976; Warmink, 2014). Therefore, they lack a stable equilibrium state. Previous studies on the River Waal have found that dune height and migration rate are positively correlated with changes in discharge (Cisneros et al., 2020; Bradley & Venditti, 2021), while dune length increases with decreasing discharge, especially over longer time periods (Lokin et al., 2022). Dunes do not readily adapt to flow conditions due to the hysteresis effect. The sediment stored in dunes has greater inertia compared to the overlying fluid; hence, there is a lag in the height, length, and migration rate of dunes (Martin & Jerolmack, 2013; Warmink, 2014). The prediction of bedform dimensions requires an understanding of three underlying factors: 1) equilibrium dimensions for a given flow; 2) the form of the underlying growth relation; and 3) the time required to reach equilibrium (Bradley & Venditti, 2019). Dredging causes bed forms to move out of equilibrium (Knaapen & Hulscher, 2002) and dunes tend to grow back to this state (Bradley & Venditti, 2021).

This study compares two dredging strategies, topping and swiping, currently used in the river Waal (Figure 3). Topping refers to the process of extracting sediment and depositing it elsewhere, typically on the other river bank. Swiping aims to move sediment from dune crests to the deeper troughs. Dredging alters the dune field by reducing the height of dunes, thus altering flow patterns and changing sediment transport dynamics (Reesink, 2018).

62 Dune dynamics have been studied extensively under various conditions, but the im-
63 pact of dredging on dune dynamics, particularly in rivers, remains limited. Previous stud-
64 ies investigating the effects of dredging on bed forms have primarily focused on differ-
65 ent environments, such as shelf seas and harbours. Campmans et al. (2021) studied the
66 impact of dredging in a navigation channel in shelf seas using an idealised process-based
67 sand wave model, focusing on the physical relations by solving the shallow water equa-
68 tions. They found that the volume of the dredging intervention plays a role in the amount
69 of time that is necessary for sand waves to reach an equilibrium state. Larger interven-
70 tion volumes lead to longer adjustment periods before sand waves stabilise.

71 Additionally, the choice of dredging technique affects sand wave behavior. When
72 comparing equal volumes of sand, swiping showed to be more effective in prolonging the
73 duration until reaching equilibrium state. Topping, however, increases the mean water
74 depth, resulting in a higher equilibrium sand wave height. The regrowth of sand waves
75 after dredging is not solely determined by the dredged volume and amplitude. Factors
76 such as bed form shape and neighboring dunes also influence this process.

77 The results of the study on the effects of dredging on sand waves are useful for the
78 investigation on river dunes. Despite some differences, these bed forms exhibit several
79 similarities. For instance, both characteristics have wavelengths that are considerably
80 greater than the water depth. They are usually oriented perpendicular to the flow di-
81 rection and can coexist with smaller and larger-scale features (Hulscher & Dohmen-Janssen,
82 2005).

83 To study the recovery of dunes after dredging activities in rivers, incorporating the
84 three-dimensional (3D) structure of the dunes is important. Bed forms in natural chan-
85 nels are predominantly 3D in plan form and show variability across the field in terms of
86 crest curvature, discontinuity and height variation (Lefebvre, 2019). A data-driven study
87 was carried out by developing a two-dimensional (2D) wavelet analysis tool to analyse
88 river dune dynamics and to capture the relevant dune parameters in terms of migration
89 and shape. The wavelet transform is able to separate waves of different wavelengths, which
90 allows for the possibility to filter out the dunes from other bed forms (Denderen, van et
91 al., 2022). Currently, one-dimensional analysis techniques have been utilised to exam-
92 ine dunes along the river axis (Mark, van der et al., 2008; Zomer et al., 2022; Lokin et
93 al., 2022). However, these models are unable to differentiate between two-dimensional
94 and three-dimensional bed form features (Gutierrez et al., 2013) and thus presume the
95 homogeneity of dunes across the river. The utilization of 2D wavelet transforms can re-
96 sult in improved scaling discrimination of bed forms (Gutierrez et al., 2013).

97 This study aims to improve the understanding of river dune behaviour in heavily
98 dredged areas of the river Waal by using a 2D wavelet tool in combination with a dataset
99 of different dredging interventions. This tool aims to address two primary research ques-
100 tions: 1) What is the post-dredging behaviour of river dunes? 2) What is the extent of
101 influence of the dredging method, i.e. topping or swiping, on these behaviours?

102 In section 2, the available dataset, the study area and the different dredging strate-
103 gies are described. Section 3 describes the methods used to identify the dune character-
104 istics. The results of the research are presented in section 4. Sections 5 and 6 contain
105 the discussion and conclusions.

106 2 Study area and data

107 The area of interest is the river Waal, the main tributary of the river Rhine in
108 the Netherlands (Figure 1). The Waal is approximately 150m wide and is used exten-
109 sively for navigation, facilitating the transport of goods between the port of Rotterdam
110 and its hinterland. The dominant mode of sediment transport is via bed load and dunes
111 are relatively symmetrical with lee angles below 10 degrees (Cisneros et al., 2020). This
112 section of the Dutch river delta is part of a maintenance contract that provides bed el-
113 evation data for this study. As part of the maintenance strategy, 10 dredging hotspots
114 are closely monitored using weekly Multibeam Echo Sounding (MBES) measurements

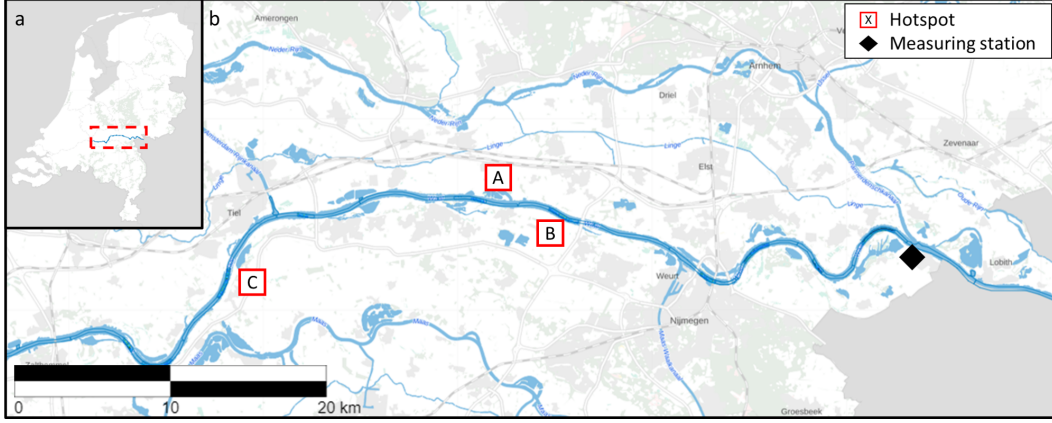


Figure 1. Overview of the river Waal. Figure *a* shows a map of the Netherlands. Figure *b* is a zoomed in map on the river Waal, showing the hotspot locations. The discharge measuring station at the Pannerdense Kop is indicated as the black diamond.

115 during the period from July 2021 until February 2023. Each hotspot covers the fairway
 116 width of 200 m over a length of 2 km. The spatial resolution of the MBES data in this
 117 study is 1x1 m (Ruijsscher, de et al., 2020). MBES measurements are taken after dredg-
 118 ing. Although not available for every dredging operation, several measurements are taken
 119 prior to dredging.

120 Discharge data are collected by Rijkswaterstaat at the Pannerdense Kop monitor-
 121 ing station (Figure 1b). The peak flow, $Q_{high} \approx 4300m^3s^{-1}$, has a return period of 1:2
 122 years. The average discharge was slightly below the 30-year median with $Q_{avg} \approx 1400m^3s^{-1}$.
 123 The lowest river discharge, $Q_{low} \approx 600m^3s^{-1}$, has a return period 1:20 years (Brenk,
 124 van et al., 2022). From the 10 monitored hotspots, three sites are selected for further
 125 examination. These sites were chosen due to the prominent presence of river dunes with-
 126 out obstructions such as fixed layers and their relative straight shape. Therefore, the in-
 127 fluence of shallow areas due to inner-bend sediment deposition is limited. The hotspots
 128 have their own site-specific characteristics, which are shown in Table 1. Site A is notable
 129 for its low dredging intensity, while site C is heavily dredged. The dredging intensity at
 130 site B is intermediate. This diverse selection allows for a comprehensive study of dune
 formation and dynamics under different levels of anthropogenic influence. Dredging oc-

Table 1. Hotspot specific characteristics, showing: location relative to river origin, topping and dumped sediment volume, and the swiped surface. During the period between July 2021 and February 2023

Hotspot	Start	End	i_b	D_{50}	Total Topping Volume	Total Dumped Volume	Total Swiped Surface	Dredging Level
	(rkm)	(rkm)	(10^{-4})	(mm)	($10^3 m^3$)	($10^3 m^3$)	(km^2)	
A	900	902	1.16	1.6	5.4	5.1	0.66	Low
B	894	896	0.87	1.6	44.2	41.6	2.28	Medium
C	918	920	1.84	1.7	119.7	105.1	4.41	High

Note. Start and end distance from origin (rkm), the bed slope (i_b), median grain sizes (D_{50}) retrieved from Damen et al., (2018).

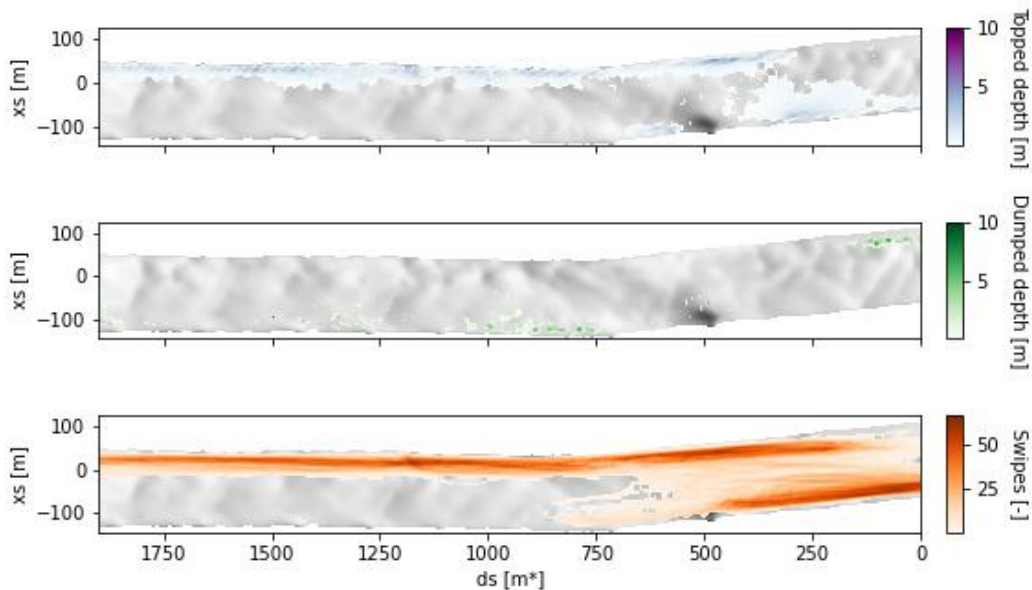


Figure 2. Heatmap of the dredging data in hotspot C between July 2021 and February 2023. The bathymetry is shown in gray, on the stream coordinates grid. Figure *a* and *b* show, respectively, the extracted and dumped volume of sediments (depth and volume is the same on a 1x1m grid). *c* shows the swiping intensity.

131 curs whenever the riverbed exceeds the dredging reference level, set by Rijkswaterstaat.
 132 This can happen weekly at certain locations. Data is collected from both the topping
 133 and swiping dredging techniques. The dredging logs for topping comprise point data with
 134 extracted sediment volumes in each 10x10m grid cell. (Figure 2a). The same applies to
 135 the dumped volume data (Figure 2b). The GPS data from the plough vessel is used to
 136 determine the intensity for swiping. Processing the GPS coordinates results in swiping
 137 tracks, which are then multiplied by the 6 m span of the plough to create a surface area
 138 that has been swiped. Swiping intensity is defined as the number of times the plough
 139 swipes a grid cell (Figure 2c). Data collection for swiping began in November 2021.

140 The initial effects of the two dredging strategies, topping and swiping, are shown
 141 in Figure 3. Figure 3a depicts that topping interventions lead to a decrease in crest height
 142 while having minimal impact on dune length. Consequently, the dune becomes less steep.
 143 The act of swiping (as shown in Figure 3b) alters both crest and trough heights. This
 144 intervention involves depositing sand removed from the crest into the trough, without
 145 extracting sediment from the system. Through swiping, both the crest and downstream
 146 trough elevation are modified, resulting in a greater reduction of dune height compared
 147 to topping with the same amount of sediment moved.

148 3 Method

149 This study analysed the behaviour of dredged dunes in five steps. The available
 150 data was pre-processed into stream coordinates first. Second, the dunes were detected
 151 using a wavelet tool. Third, the dunes' migration was determined, followed by the de-
 152 termination of relevant dune parameters as the fourth step. Last, the tracking of the dunes
 153 over time was carried out. Figure 4 gives a representation of these steps.

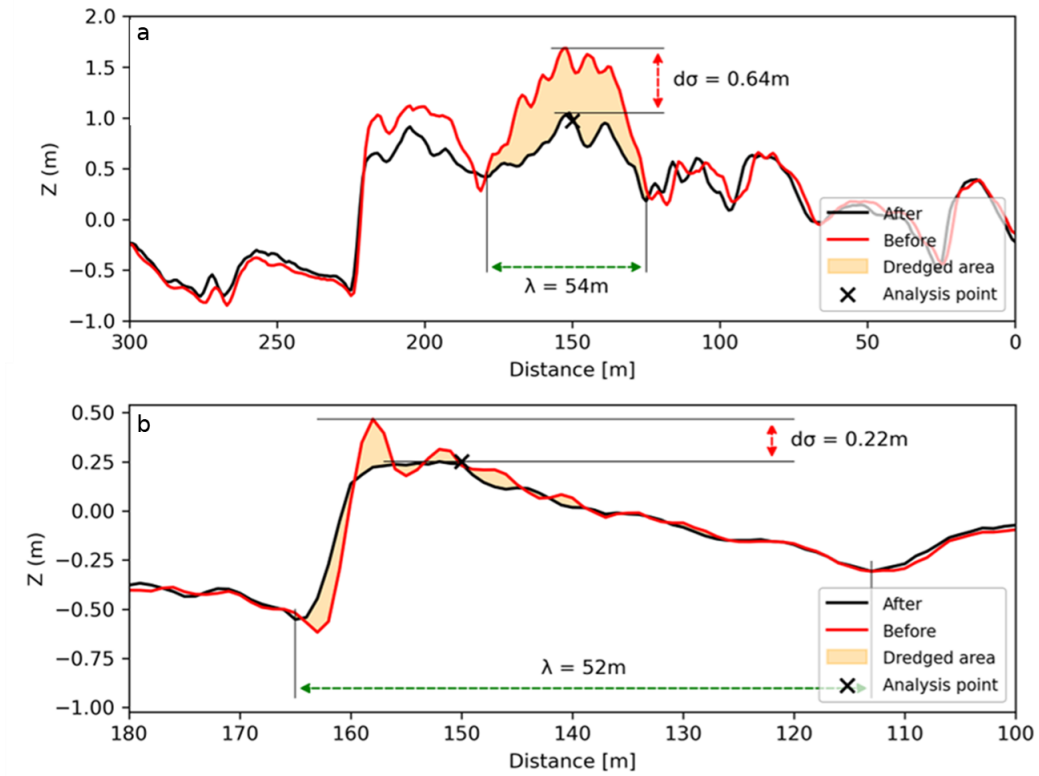


Figure 3. Figure *a* shows an example of topping, where $\approx 27\text{m}^3\text{m}^{-1}$ sand is dredged from the dune. Figure *b* shows an example of swiping, which moved $\approx 2.5\text{m}^3\text{m}^{-1}$ sand. The elevation profiles are taken from the pre- and post-dredge measurements.

154 The MBES and dredging data are pre-processed into rasters of stream coordinates
 155 (Legleiter & Kyriakidis, 2006), for further processing with the dune analysis tool. Stream
 156 coordinates are defined by the distance along the river axis (ds) and the distance across
 157 the river (xs). ds is considered positive in streamwise direction. xs is negative at the left
 158 river bank and increases towards the right bank. The river axis is set as $xs = 0$.

159 3.1 2D Wavelet tool and dune detection

160 The analysis makes use of the two-dimensional continuous wavelet transformation
 161 (CWT), using the 2D Ricker wavelet (Mexican Hat). This approach is based on the prin-
 162 ciples of continuous wavelet transform (Torrence & Compo, 1998). The 2D CWT trans-
 163 forms spatial data (x, y, z) into a space of location (a, b) and wavelength (λ). This results
 164 in the amount of energy that is present for each wavelength at any location (Booth et
 165 al., 2009). The transformation allows for examination of the data at different levels of
 166 spatial scales, ranging from coarse approximations to fine-scale details. Therefore, the
 167 wavelet transformation allows for filtering and visualisation of the bathymetry for spe-
 168 cific wavelengths of bed forms (Struble et al., 2021).

169 The 2D CWT is a convolution of the elevation signal (z), and a wavelet function
 170 (ψ) (Booth et al., 2009).

$$C(s, a, b) = \frac{1}{s} z(x, y) \cdot \psi \left(\frac{x - a}{s}, \frac{y - b}{s} \right) \quad (1)$$

171 Here, $C(s, a, b)$ represents the wavelet energy. A large wavelet energy corresponds to a
 172 better match between the wavelet function and $z(x, y)$, at each node for a wavelet scale
 173 (s). A larger wavelet scale corresponds to larger wavelengths, and vice versa (Torrence
 174 & Compo, 1998; Booth et al., 2009; Struble et al., 2021). The 2D Ricker wavelet func-
 175 tion, ψ_R , is considered appropriate for this analysis as it was used previously for topo-
 176 graphic purposes (Booth et al., 2009; Struble et al., 2021) and has good localisation in
 177 space (Hernandez-Hernandez et al., 2021). Although the Ricker wavelet is known to have
 178 a limited frequency bandwidth (Torrence & Compo, 1998), this characteristic does not
 179 significantly hinder the analysis of river dunes, particularly as the primary focus is on
 180 identifying the locations of crests and troughs. The 2D Ricker wavelet is a brief oscil-
 181 lation and is given as:

$$\psi_R(x, y) = (2 - x^2 - y^2) \cdot \exp \left[-\frac{x^2 + y^2}{2} \right] \quad (2)$$

182 Dunes in the study area typically have wavelengths ranging from 20-150 m during me-
 183 dian and high flows (Ruijsscher, de et al., 2020). However, the dataset shows discharges
 184 slightly lower than median, leading to wavelengths potentially exceeding 150 m. Con-
 185 sequently, the dune signal is reconstructed for wavelengths between 20 and 300 m, ex-
 186 cluding the smaller ripples (Frings & Kleinhans, 2008; Zomer et al., 2022)) and larger
 187 bed features (Ruijsscher, de et al., 2020).

188 To reconstruct the dune field, the wavelengths are converted into their wavelet scales
 189 by using a Gaussian second-order derivative ($m=2$) (Torrence & Compo, 1998). (See Equa-
 190 tion 3). The lower and upper bound wavelengths were structured into 42 suitable scales,
 191 producing satisfactory outcomes while limiting the computational time. A base-2 log-
 192 arithmic scale is used to separate the scales (Torrence & Compo, 1998).

$$s = 2\pi\lambda/\sqrt{m + 0.5} \quad (3)$$

193 The signal resulting from each scale was combined to fully reconstruct the dune field,
 194 enabling the detection of individual dunes. Dunes were detected by their crest locations,
 195 which were identified based on the local maxima in the reconstructed signal. Figure 4c
 196 shows an example of the crest lines on a reconstructed signal.

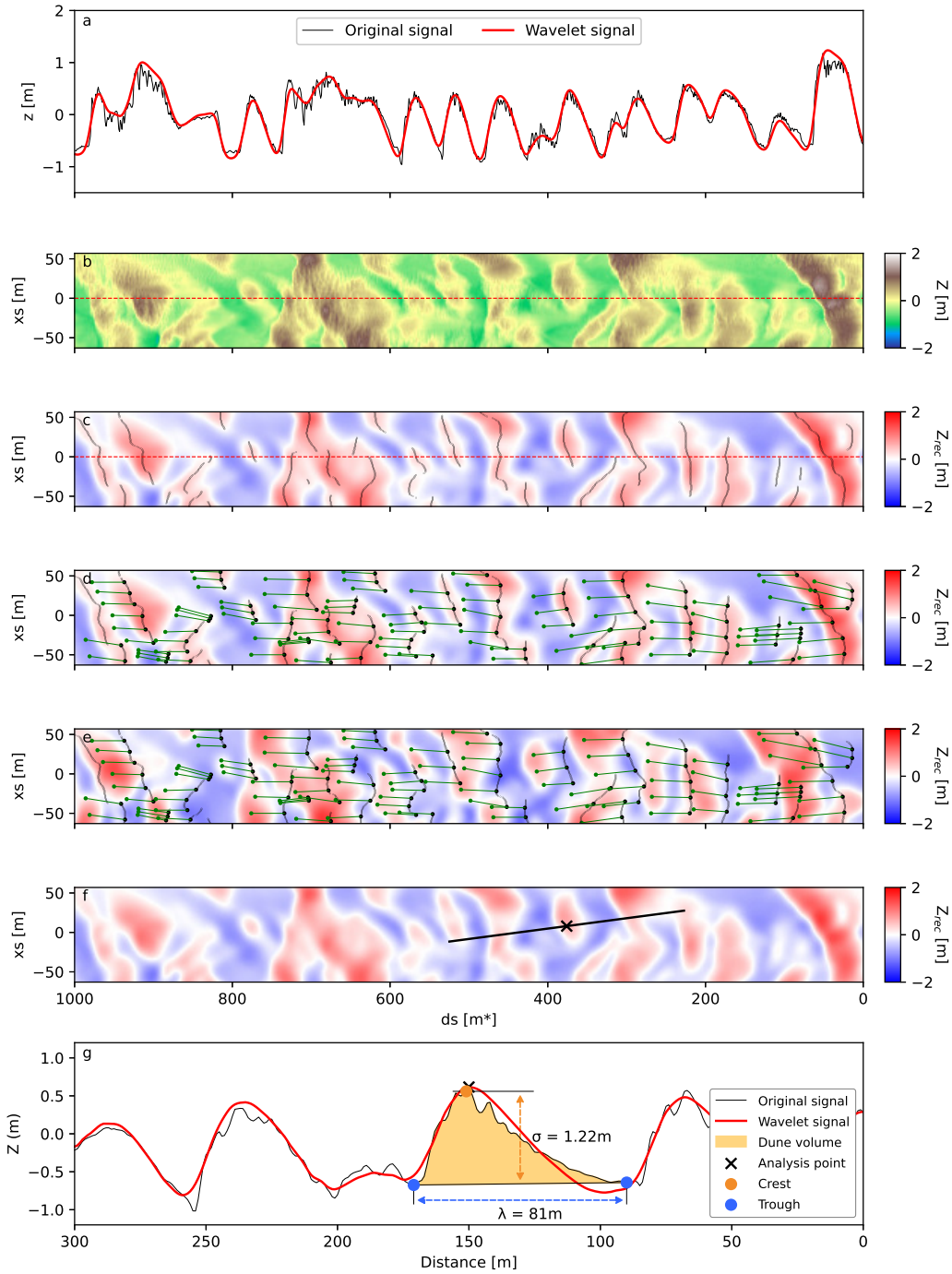


Figure 4. An overview of the steps carried out by the wavelet tool. Figures *a-c* show the 2D CWT for 1 km river using wavelengths of 20-300 m. Figure *a* shows the 1D bed profile along the river axis, comparing the original and reconstructed wavelet signal. Figure *b* is the 2D representation of the river bathymetry (Z) for comparison with the 2D reconstructed wavelet signal (Z_{rec}) in Figure *c*. The initial crest locations are plotted here as well. Figures *d* and *e* show dune migration in hotspot A, resulted from the Spatial Cross-Correlation for a period of 8 days. Black dots are the analysis points on the dune crests at $t=0$ (Figure *d*); the green dots indicate the highest correlation at $t=1$ (Figure *e*); and the green line shows the displacement. Figure *f* shows the location of the analysis point on the wavelet signal with a transect of 300 m. Figure *b* shows the wavelet and original elevation signal along the transect, in combination with the locations of the crest and troughs. The orange arrow indicates dune height, while the blue arrow indicates dune length.

197

3.2 Dune migration

198

199

200

201

202

203

204

205

The migration of dunes is determined based on the displacement of crest locations between consecutive measurements (Figures 4d,e), which are calculated using a 2D spatial cross-correlation (SCC) method (Duffy & Hughes-Clarke, 2005; Meijden, van der et al., 2023). This approach assumes that the bed elevation profile shifts downstream between two time-based measurements while the shape of the dunes remains relatively constant (Lokin et al., 2022). Consequently, this approach yields displacement values in both the ds and xs directions. The determination of the mean dune celerity was feasible with this data set due to frequent measurements (Lokin et al., 2022).

206

207

208

209

210

211

Performing the 2D SCC is computationally intensive when performed for each crest location. To reduce computation time, at least three analysis points are defined along each dune crest line. The distance between each analysis point is at most 20 m. Smaller dunes are assigned at least three analysis points; thus, each dune is analysed at several locations to show the spatial variability along the dune (Meijden, van der et al., 2023).

212

213

214

215

216

The displacement values are divided by the time intervals between measurements to determine dune celerity at each analysis point. Lower and upper bounds for displacement are introduced to remove outliers and account for spatial and temporal variations in migration directions and rates. These limits are defined as two times the standard deviation of the mean migration directions and rates, and they serve to reduce the uncertainties in river dune migration (Le Coz et al., 2022).

217

3.3 Dune shape

218

219

220

221

222

223

224

225

226

227

228

229

230

Transects are drawn at the analysis points in the direction of dune migration as previously determined (Le Coz et al., 2022) (Figure 4f). The transect length is set to the largest wavelength considered in the wavelet transformation so that the dunes are completely covered. The highest points (crests) and lowest points (troughs) are identified for each transect based on the local maximum and minimum values around the analysis point. A crest is defined as the highest point in the original profile closest to the highest point's location in the reconstructed profile (Lokin et al., 2022). The local minimum points closest to the crest are found upstream and downstream to determine dune troughs. Smoothing is performed using a Savitzky-Golay filter (Savitzky & E, 1951) with a filter span of 41 data points (approximately 41 metres), fitting a third-order polynomial to remove overlapping ripples from the original bed profiles while preserving the shape of the dunes. Only local maxima, at least 0.1 m above the nearest local minimum, are included as crest locations (Lokin et al., 2022).

231

232

233

234

235

236

237

Based on the trough and crest locations, the dune shape parameters are determined (Figure 4b). Dune length (λ) is defined as the horizontal distance between two consecutive troughs (Lokin et al., 2022); Dune height (σ) is defined as the vertical distance between a crest and the average elevation of the two adjacent troughs (Zomer et al., 2022); the aspect ratio ($\psi = \sigma/\lambda$) is defined as the dune height over the dune length; and the dune lee slope angle (α). This angle is defined as the mean slope of the middle 2/3th part of the dune lee slope (Mark, van der et al., 2008).

238

3.4 Dredging analysis

239

240

241

242

243

244

245

246

Dune tracking findings facilitated four dredging analyses: first, an analysis of the entire dune field in the study area; second, an analysis of the immediate effects of dredging by comparing data collected immediately before and after dredging; third, an analysis of the initial response of the dunes to dredging; and finally, a long-term analysis of the evolution of the dredged dunes.

The 2D wavelet tool analyses the entire field to derive information on all dunes at the selected sites. The dune height, length, and celerity are examined based on river discharge and the variation in dredging intensity between sites.

247 The analysis of the direct impacts of dredging distinguishes between the topping
 248 and swiping methods. The difference in height resulting from the intervention is deter-
 249 mined by using pre- and post-dredge MBES measurements. To compare the dune pro-
 250 files, the migration of dunes between these measurements has been accounted for.

251 Dune development was evaluated after the dredging process by tracking the dunes
 252 for a week and comparing them with flow conditions and unaffected dunes to understand
 253 their initial behaviour after dredging. Dredged dunes were tracked over 50 days to ex-
 254 amine their behaviour over a longer period. As dredging is a frequent occurrence, some
 255 dunes may be re-dredged during the monitoring period. Tracking times for these dunes
 256 are shortened to show undisturbed dune development in the dataset. This allowed for
 257 the determination of development parameters such as growth rate (σ/σ_0) and migration
 258 speed (c).

259 4 Results

260 4.1 Dune analysis

261 The dune analysis was done for the entire dune field in the three selected study sites.
 262 This gives insight into the relation between the dune parameters and the river discharge
 263 in time (Figure 5).

264 The height of the dunes corresponds to the variations in river discharge at all sites,
 265 (Figures 5a-c). This relation is especially noticeable during high discharges, such as the
 266 flood wave in February 2022, as dune height rises with discharge. Likewise, as the dis-
 267 charge subsequently decreases, dune height also reduces.

268 From January to May 2022, three significant flow peaks were observed. In contrast,
 269 the dune height exhibits only a single peak during this period. This indicates that dune
 270 height does not adapt to flow changes at the same rate and lags behind the new flow con-
 271 ditions, confirming previous findings on hysteresis (Martin & Jerolmack, 2013; Warmink,
 272 2014).

273 Dune heights in site A show a larger difference between the dune heights during
 274 high and low flow than the dune heights in site B and C. This observation suggests that
 275 dunes are less sensitive to height changes in areas with a higher degree of dredging ac-
 276 tivity. Site A had the highest average dune height during the analysed period, while Site
 277 B had the lowest average dune height.

278 Dune length is relatively constant over time (Figures 5d-f). Despite being minimal,
 279 Site A displays the largest variation in dune length, whereas the dune length in Site C
 280 is most stable. Specifically, a slight rise in dune length is observed during the low dis-
 281 charge period in August 2022. The average dune length during the whole analysed pe-
 282 riod is relatively similar for all sites.

283 The celerity shows a positive relation with flow across all sites, as shown in Fig-
 284 ures 5g-i. This is evident from the increasing celerity rates observed between November
 285 2021 and January 2022. A difference in average dune celerity between the locations is
 286 observed over the 1.5 year period, with the highest celerity in the hotspot with the low-
 287 est dredging intensity and lowest in the hotspot with the largest dredging intensity.

288 The topping intensities throughout the analysed period are shown in Figures 5j-
 289 l. The most topping activity took place after the discharge peaks. During falling water
 290 levels, the larger dunes that did not fully adapt to the new flow conditions yet, can lead
 291 to the formation of shallow areas. Swiping data tracking began in November 2021, (Fig-
 292 ures 5m-o). The pattern of swiping intensities is similar to that of topping, suggesting
 293 a logical correlation since most dunes that undergo topping also experience swiping. Swip-
 294 ing occurs more often than topping while discharge is increasing, for example between
 295 November 2021 and February 2022. The intensity of both topping and swiping is posi-
 296 tively related to dune height.

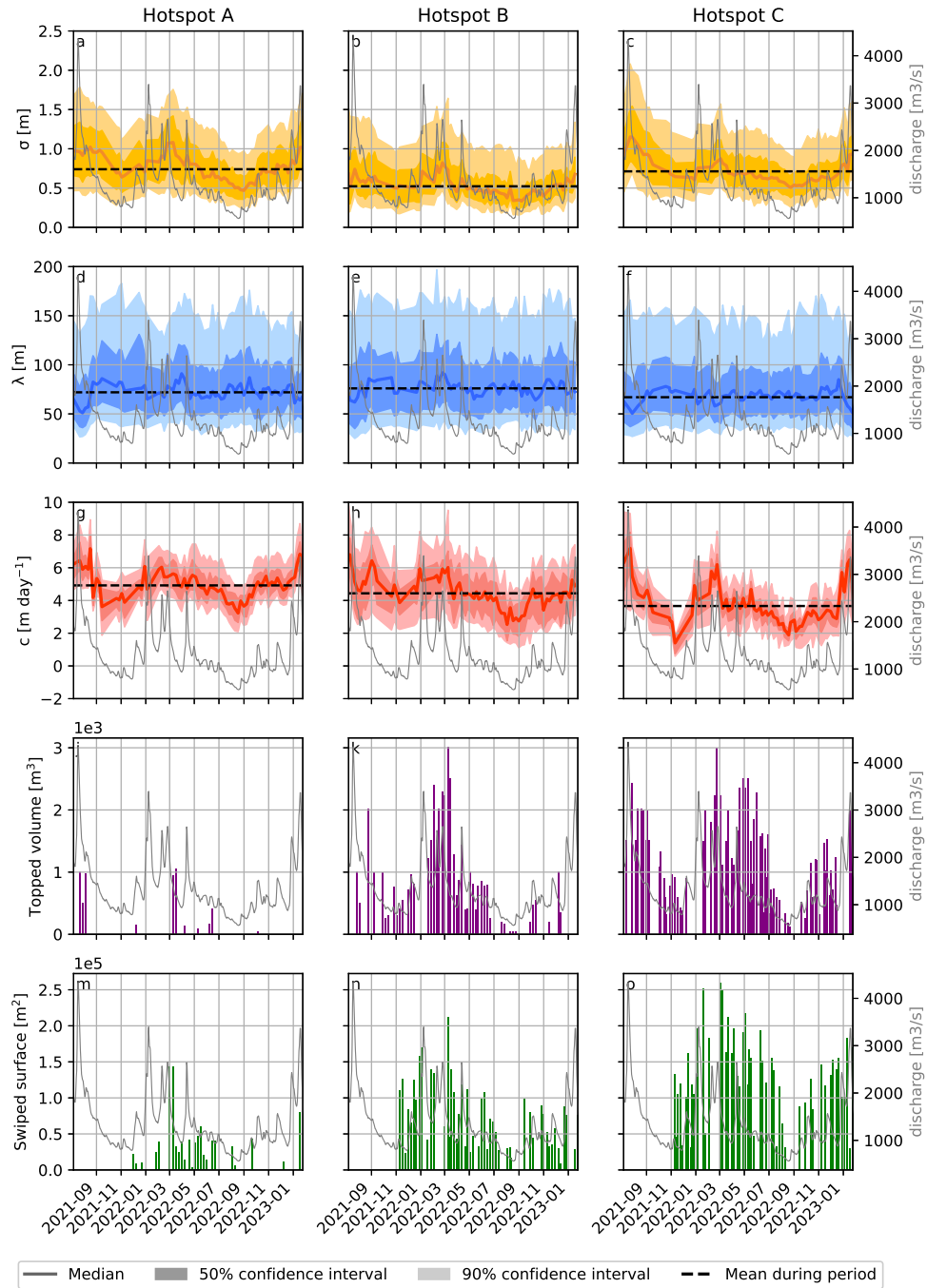


Figure 5. Overview of dune parameters and dredging intensity during the period between August 2021 to January 2023. The columns indicate hotspots A, B and C and river discharge is shown on the secondary axis of each figure. The medians for dune height (Figures a-c), dune length (Figures d-f) and dune celerity (Figures g-i) are plotted with their confidence intervals. The dashed black line indicates the mean during the whole period. The topped volumes in each hotspot is plotted in Figures j-l with the swiped surfaces shown in Figures m-o.

297

4.2 Effect of dredging on dune characteristics

298

299

300

301

302

303

304

305

306

This section examines the direct effects of the topping and swiping dredging strategies by comparing the shape of the dunes before and after dredging. The analysis is based on pre- and post-dredge measurements taken approximately 3-30 hours apart. Figure 6 illustrates the impact of the dredging intensity of both swiping and topping on the changes in dune height and length immediately after dredging. Here, each dune is examined separately, with an average dune height and length calculated for all of the analysis points along each crest. The topping intensity is defined as the average sediment volume extracted per metre along the crest of the dune. The swiping intensity is defined as the average number of swiping movements per metre along the dune crest.

307

308

309

310

311

312

313

314

315

316

317

318

In Figures 6a and b, the change in dune height ($d\sigma$) is presented. Both topping and swiping techniques are expected to result in a reduction of dune height. Despite the few occurrences of positive values, most dunes demonstrate a significant negative change in height for both topping and swiping techniques. The fitted lines exhibit different steepness, but it is difficult to compare the results for topping and swiping because of the different way of measuring dredging intensity for these methods. As is anticipated, the p -values (< 0.01) indicate a significant correlation between dredging intensity and the decrease in dune height. Both dredging types decrease the dune height significantly, however the variation in dune height change is also quite large. Therefore, the change in dune shape may not be attributed solely to dredging intensity, indicating the possible contribution of other fluvial processes during the period between pre-dredging and post-dredging measurements.

319

320

321

322

323

324

325

Figures 6c and d illustrate the impact of dredging intensity on the alteration in dune length ($d\lambda$). Regarding topping, the alteration in dune length varies markedly, showing both positive and negative changes. Regarding swiping, $d\lambda$ displays greater consistency. Overall, the average alteration in length is slightly positive, irrespective of dredging intensity. There is no significant correlation ($p > 0.01$) between dune length and dredging intensity, suggesting that neither topping nor swiping intensity can be attributed to changes in dune length.

326

327

328

329

330

331

On an individual dune, swiping can result in a minor lengthening of the dune, due to sediment deposition in the downstream trough. However, when several consecutive dunes along one swiping track are analyzed, the location of the upstream trough of an individual dune also changes by the swiping of the upstream dune. Resulting in minimal changes in dune length. The dune length is not expected to be affected by topping. As a result, dune length will remain relatively constant for both topping and swiping.

332

4.3 Initial response after dredging

333

334

335

336

337

338

339

340

341

342

343

344

Figure 7 shows the initial change in dune behaviour during the first week after dredging at hotspot C for different flow conditions. Since the period between measurements is not precisely one week, the dune behaviour is expressed by the average daily growth for both height ($d\sigma/dt$) and length ($d\lambda/dt$).

No relation is observed between either $d\sigma/dt$ or $d\lambda/dt$ and discharges (Figures 7a-c). Growth and decay values appear to be roughly equivalent when comparing unaffected and dredged dunes, with a median located at $d\sigma/dt = 0$. Of the observed dunes, unaffected ones show the most variability in growth, while topped dunes exhibited the least. A comparable observation applies to the connection between the change in dune length and discharge. The results suggest that both swiped and, in particular, topped dunes are more stable than regular unaffected dunes and develop more gradually in the immediate period after the intervention.

345

346

347

348

349

A significant positive correlation exists between dune celerity and flow for both dredged and unaffected dunes ($p < 0.01$), as indicated by the fitted line in Figures 7g-i. The fitted line is derived from the point data of individual dunes. The relation between dune celerity and discharge is similar for both unaffected and dredged dunes. The mean migration rates are comparable for unaffected and topped dunes, whereas the celerity of

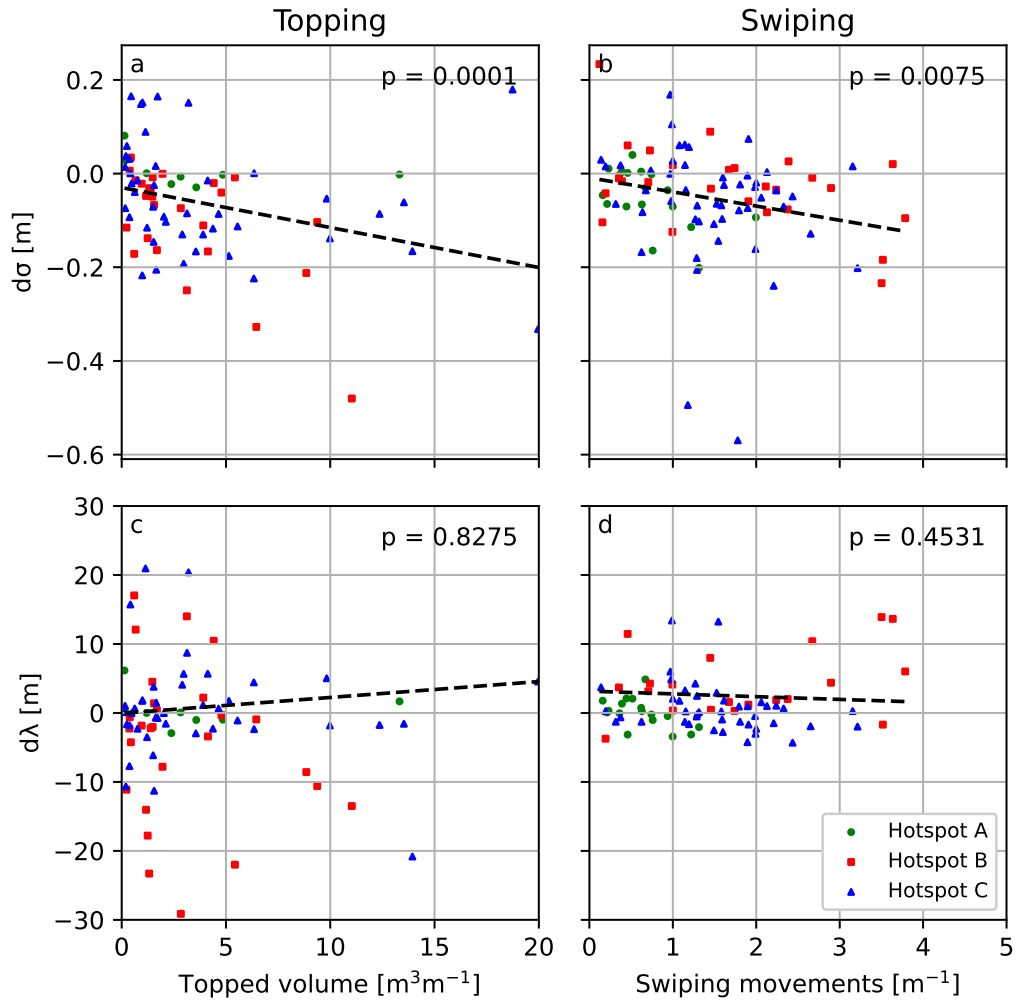


Figure 6. Direct effect on dune shape for dredging methods, topping and swiping, compared to dredging intensity. Each data point represents a single dune. Shape differences are compared between pre- and post-dredge measurements, at most 30 hours apart. Figures *a* and *b* show the difference in dune height, while Figures *c* and *d* show the difference in dune length. The p -value is shown in each figure, indicating the significance of the correlation between the variables.

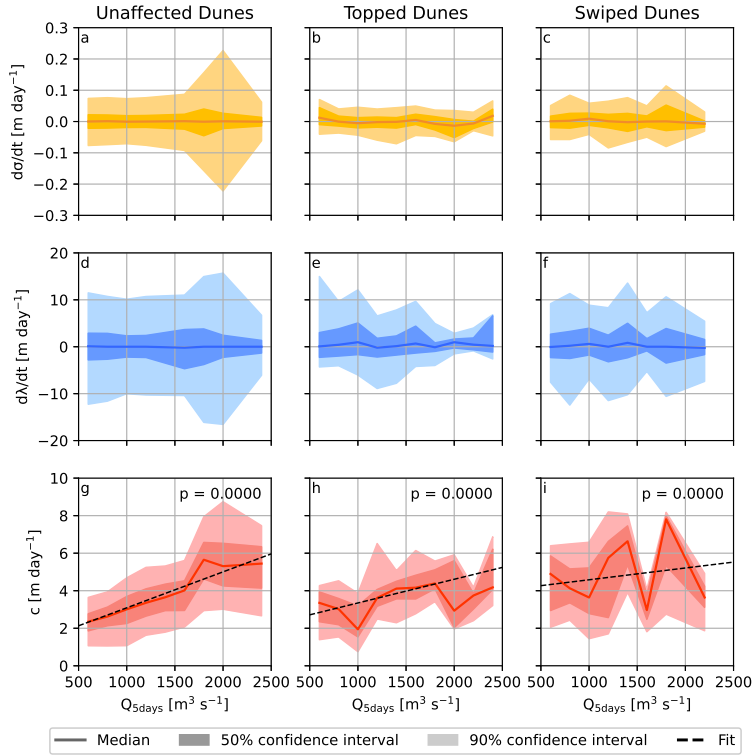


Figure 7. The initial behaviour of the dunes during the first week after dredging. The variables related to dune behaviour are plotted for unaffected, topped and swiped dunes against the average five-day mean discharge (Q_{5days}). Figures *a-c* show the daily growth in height; the daily growth in length is plotted in Figures *d-f*; and the average celerity is shown in Figures *g-i*. The dashed lines in the celerity figures represent the fit for the relation with flow. The corresponding *p*-value indicates the significance of the relation.

350 swiped dunes is marginally larger. Celerity for swiped dunes show a downward spike at
 351 $Q_{5days} = 1600m^3s^{-1}$. This is likely caused by a limited set of dredging data for $Q_{5days} >$
 352 $1500m^3s^{-1}$. The celerity values were captured from a period of decreasing discharge, where
 353 dunes were adjusting to flow conditions, resulting in a lower celerity.

354 **4.4 Dune behaviour after dredging**

355 Dredging causes bed forms to move out of their dynamic equilibrium and dunes
 356 tend to grow back to this state (Bradley & Venditti, 2021). Figures 8a-f show the mean
 357 growth ratios of dune height, length and celerity over a period of 50 days. As a result
 358 of topping, the height and length of the affected dunes grow. Topping shows larger growth
 359 ratios (σ/σ_0) for larger values of dredged volume. More dredged dunes are pushed fur-
 360 further out of equilibrium and grow faster and therefore have a larger rate of change to adapt
 361 to the equilibrium than the dunes that were subjected to less dredging. Dune growth
 362 increases gradually over time, with a slower growth rate observed in the first few weeks
 363 following dredging. It is notable that the dunes studied do not grow when only a small
 364 portion of the dune is topped. When topping volumes are increased, the growth ratio
 365 appears to be larger than that of swiping after 50 days. Regarding swiping, the dune growth

ratio typically remains relatively stable at around $\sigma/\sigma_0 = 1$. However, with a larger swiping intensity, the dredged dune tends to grow as well. It is challenging to compare the intensity of topping and swiping due to the use of different measuring units. Nevertheless, the highest growth ratios for swiping are lower than those for topping after 50 days. This suggests that swiping may be more effective for larger dredging intensities, as dunes recover at a slower rate.

The length of topped dunes shows values above 1, suggesting growth scaling. It appears that the growth of topped dunes follows a scaling pattern as dune length seems to increase with dune height. The swiped dunes maintain a stable length, with an average of $\lambda/\lambda_0 = 1$. Although there's some variation in λ/λ_0 values among all data points, different swiping intensities do not seem to be the main cause. The increase in celerity for topping is greater than 1, indicating acceleration of the dunes. Over time, dunes tend to accelerate combined with an increase in both height and length. Following dredging, celerity may be low, as dunes have a flattened shape and are less susceptible to erosion. For lower swiping intensities, the celerity remains fairly constant, which aligns with the stable patterns observed in both dune height and length.

The daily growth ratio ($\sigma/\sigma_0/day$) for topping and swiping at hotspot C during 2022 is shown in Figures 8g and h. There is a significant variation in growth ratios between individual dunes at any given time. The range of growth, as shown by the confidence interval, indicates that the dunes impacted by dredging are not all growing or shrinking at a similar rate.

For topping, the daily growth mostly follows the pattern of the unaffected dunes. Between March and April the decline of topped and unaffected dunes is comparable. This is largely due to the relatively sudden drop in discharge. A peak in growth can be observed around November, which may be caused by the sustained increase in discharge over the last few weeks. After this period, the topped dunes show greater growth than the unaffected dunes. During the period of decreasing river discharge in April and December, dune growth is lower after swiping compared to unaffected dunes. Dune growth increases slightly compared to unaffected dunes during stable discharge periods from May to July and during the early stages of low flow in September.

5 Discussion and reflection

5.1 Reflection on dune dynamics

The analysis of the dunes in Section 4.1 revealed a positive correlation between dune height and celerity with discharge. This aligns with prior research on river dunes in natural rivers (Cisneros et al., 2020; Bradley & Venditti, 2021). Section 4.1 yields the following conjectures on dredging and dune dynamics. First, locations with higher dredging intensity show less significant fluctuations in dune height. Dredging leads to a reduction in dune height (Section 4.2). Thus, areas with more frequent dredging activities will have a comparatively lower peak of average dune height.

Dredging may counteract the tendency of dunes to lengthen during periods of low flow. Previous research found a stronger negative correlation between dune length and discharge (Lokin et al., 2022), but in this study dune length remained relatively constant. From Figure 5 it can be observed that, although minimal, dune length increased most in the least dredged site during falling river discharge. If dredging does play a role in reducing variation in dune length, it is likely to be minimal as no direct relation was found between dredging and dune length (Section 4.2). A more probable explanation is the duration of low flow, which was, in this study, only briefly compared to the 4-month duration observed in Lokin et al. (2022).

Figures 5g-i suggest that dredging impacts the migration rate of dunes, slowing it down. This was indicated by the decreasing mean dune celerity with increasing dredging intensity between sites A, B and C. Dredging causes a reduction in dune size and smaller bed forms usually migrate faster (Lee, 2022). Nevertheless, dredging has a greater im-

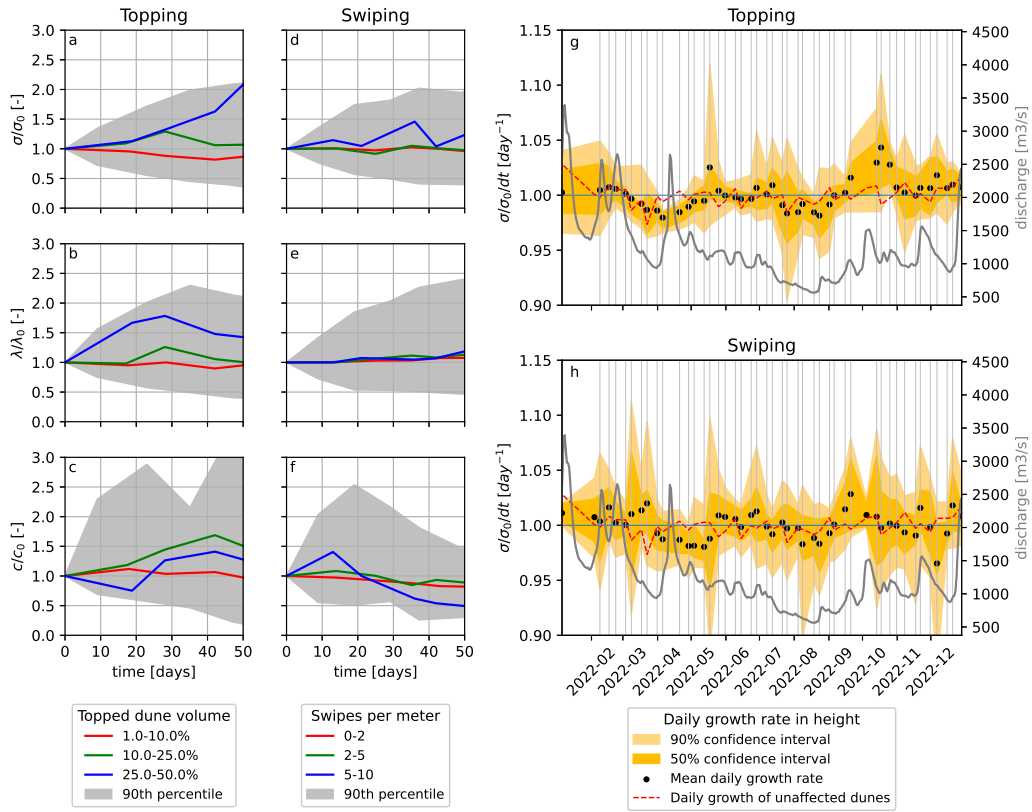


Figure 8. Development of dredged dunes over time. *a-f* show the growth of the main dune parameters against time, where $t=0$ is the first measurement after dredging. The coloured lines indicate median growth ratio for the intensity of the dredging method; extracted percentage of the dune volume for topping and average plough movements per m² dune surface. *g* and *h* show the daily growth s ($H/H_0/day$) in hotspot H during 2022 for dunes affected by dredging within the last 5 weeks. The red line represents the unaffected dunes.

418 pact on the shape rather than the scale of the dunes. This flatter shape may lead to a
419 streamlined dune with reduced erosion on the stoss side, which may result in lower bed
420 load transport as well as lower dune celerity.

421 **5.2 Initial effect of dredging interventions on dune shape**

422 The study examines the direct change in height and length of topping and swiping
423 due to dredging, through a comparison of pre- and post-dredge measurements. A cor-
424 relation between dune height reduction and dredging intensity was found for both dredg-
425 ing methods. The changes in length cannot be directly related to the dredging activi-
426 ties. Despite this correlation, there is a significant degree of variation. Therefore, other
427 factors are also likely to influence the altered dune shape after dredging. This is, addi-
428 tionally, supported by the variations in dune length changes after topping. Three poten-
429 tial sources of this variation in the comparison of dredging intensity and dune shape de-
430 formation are the following: 1) natural bed development that takes place between pre-
431 and post-dredging measurements, 2) changes in sediment transport conditions caused
432 by the dredging, and 3) if the dune undergoes significant deformation that makes it un-
433 detectable.

434 **5.2.1 Natural bed development**

435 The interval between pre- and post-dredge measurements varied from 3 to 30 hours.
436 Measurements revealed migration of up to 7 metres during this time, indicating flow ve-
437 locities exceeded the threshold for incipient movement. Despite the migration being largely
438 accounted for, natural fluvial processes can still cause deformation through sediment ero-
439 sion and deposition. Secondary bed forms such as superimposed ripples may amplify these
440 processes (Zomer et al., 2021). Moreover, navigation activities on the river Waal could
441 potentially increase the transport capacity and result in ship-induced turbulence and ero-
442 sion. Since dredging activities concentrate on areas that are crucial for navigation, the
443 dredged dunes are particularly susceptible to these impacts in this area.

444 **5.2.2 Sediment transport**

445 Dredging may affect the natural dynamics of a river system and significantly im-
446 pact sediment transport. After sediment is extracted from a river, a layer called resid-
447 ual sediment remains on the river bed (Patmont, 2018). This sediment is made up of dis-
448 lodged or suspended particles that increase sediment transport in the river. As a result
449 of dredging activities, sediments previously settled or buried can be re-suspended into
450 the water column, leading to increased suspended and bed-load sediment transport im-
451 mediately after dredging. Dredging-induced turbulence can increase sediment mobility,
452 resulting in increased erosion (Laleye et al., 2019). The higher sediment transport could
453 cause further erosion of the dune immediately after dredging, which is a possible expla-
454 nation why dune deformation is not zero at minimal dredging intensities. This is shown
455 by the trend lines in Figures 6a and b, which do not pass through the origin, with heights
456 starting to decrease after a few centimetres for both topping and swiping.

457 Sediment extracted during dredging is usually transported and disposed of elsewhere.
458 The dredged sediment volume is comparable to the deposited volume in the hotspots (Ta-
459 ble 1). This indicates that the dredged sediment is deposited on the opposite river bank.
460 Nonetheless, it takes a considerable amount of time for the dredged sediment to settle
461 on the river bed (Ding et al., 2022). Such removal can disturb the natural balance of sed-
462 iment within the river, which may affect the riverbed erosion and the deposition patterns
463 downstream (Cox et al., 2021).

464

5.2.3 Dune detection and data

465

466

467

468

469

470

471

472

473

474

475

476

477

478

479

480

481

482

483

484

485

486

487

Differences in dune shape may be a result of the dune detection method used. It is possible that dunes, which were detected as complete structures initially, become reduced in size, leading to a situation where they no longer satisfy the settings of the analysis tool. In that scenario, the tool identifies the dune as part of a neighbouring one, altering the locations of the troughs. This leads to a substantial change in dune length. Another scenario is where dunes are dredged in a manner that gives the appearance of dune splitting, resulting in shorter dune lengths. Swiping moves the sediment, reducing smaller perturbations and smoothing the dune (Figure 3). Topping is a rougher technique, which leaves greater disturbances on the bed. The larger perturbations are a source of irregularities in the detection method. Which is why the impact of dredging on the variability of dune length is more noticeable with topping.

The uncertainties associated with the available dredging data pose a challenge in establishing a clear relationship between dredging intensity and dune deformation. Uncertainties in the topping data arise from grid cell resolution of the bed elevation data (x,y), which is 10 times larger than that of the swiping data. This difference in resolution can introduce small scale inaccuracies in the data. Sediment volume determination involves manual logging, which introduces a margin of error. This process can lead to variations in recorded values and affect the accuracy of volume calculations. The location and frequency of topping is considered to be reliable and provides valuable information for analysis. The accuracy of topping data depends on the plough's GPS. Although GPS devices can be fairly accurate, it is widely recognised that they have a margin of error (Cocard et al., 1999). This potential error in GPS readings can affect the accuracy of the swiping data used to assess dredging impacts.

488

5.3 Dune evolution after dredging

489

490

491

492

493

494

495

496

497

498

499

500

501

502

503

504

505

506

507

508

509

510

511

512

513

514

515

516

The study focused on the dunes in dredged areas, considering their initial response to the intervention and their long-term development over a 50-day period.

Both swiped and especially topped dunes were observed to show minimal deviation in growth rates during the first week after dredging. This suggests that they are more stable than regular, unaffected dunes and are less susceptible to flow and sediment dynamics. This implies that they are more stable and less susceptible to flow and sediment dynamics than regular unaffected dunes. Dredging reduces the height of dunes, while keeping their length relatively stable. As a result, the dunes have a lower steepness (σ/λ), which most likely leads to lower lee angle slopes. One potential explanation for this is that flatter dunes could produce lower turbulence than steeper, unaffected dunes. This lowers the flow resistance caused by the dune form roughness (Cisneros et al., 2020). The reduced flow resistance poses more challenges for sediment deposition on the dredged dune and slows down its growth.

In terms of long-term dune behaviour, it was observed that dunes grow in height after both topping and swiping activities. Since dredging leads to a deviation from the equilibrium state, dune height would increase as it develops back towards equilibrium (Bradley & Venditti, 2021). This was especially noticeable for higher dredging intensities, where dune height is most affected. As flow conditions are constantly changing, it is difficult to determine when dunes have regrown to reach their equilibrium height. After 50 days, topping exhibited larger growth ratios compared to swiping, indicating that swiping is the most effective method to keep dunes away from equilibrium. For their tidal sand wave study, Campmans et al. (2021) demonstrated comparable results. Disruptions on the dune surface could be a potential reason for the slower development of swiped dunes. The swiped dunes showed fewer perturbations or secondary bed forms than the dunes that were topped, after the intervention took place. These disturbances may contribute to growth.

The analysis results have made it challenging to quantify the growth relation of dunes following the dredging intervention. Earlier studies proposed a relation for the recovery

of sand waves based on their amplitude in the form of a Landau function (Knaapen & Hulscher, 2002). This S-shaped curve was not directly observed through the river dune analysis. The probability of river dunes following the same S-shaped curve is low given the variable forcing and the influence of other bed forms migrating at different rates. The growth ratios of high-intensity topping (Figure 8a) hint at a development that looks like the early stages of the Landau function. Longer tracking times of dredged dunes could potentially provide further insights. Unfortunately, such an investigation was not possible with the current dataset. To achieve that, it would be necessary to obtain dredging data over a longer period of time, during which the same dunes would not undergo further dredging.

The results show that regrowth of dunes after dredging is more than only a function of time, dredging intensity and discharge. Factors such as turbulent flow fields, dune morphology, sediment transport and secondary bed forms would influence regrowth significantly (Reesink, 2018; Naqshband et al., 2021).

5.4 Efficient dredging

Efficient dredging involves optimising dredging operations to ensure the river's primary function of navigation, with a focus on factors such as cost-effectiveness and emission reduction. Specifically in the case of the Waal, efficient dredging is defined as maintaining safe navigation depths while minimising dredging time.

This study showed that topping has a more pronounced effect on immediate dune height reduction than swiping. Comparing the intensities of topping and swiping is challenging due to different units of measurement. However, by assessing topping volume and swiping movements relative to their respective maximums within a dredging event, it appears that topping may have a more consistent influence on immediate dune height reduction. Conversely, swiping may be more effective in the long term as dunes tend to grow more slowly and swiping is less disruptive to the sediment balance.

Compared to multiple dredging events, a single large over-depth dredging operation is more time-efficient. To ensure the minimum navigable depth for a longer duration, a single dredging operation requires higher dredging intensity. However, it has been observed that dredging larger volumes of sediment results in higher growth rates, potentially increasing total dredging volume during maintenance. Multiple dredging events with lower intensity have less impact on the system's equilibrium, showing significantly lower dune growth ratios.

Dredging takes place when the flow decreases (Figures 5j-o), presumably because the reduction in dune height lags behind the changes in flow, causing shallow areas. This may be less time-effective as dune heights tend to decrease naturally. Nevertheless, dredging during these periods makes the dunes closer to reaching equilibrium and may cause dune development to slow down more quickly.

Designing an efficient dredging strategy is a challenging task due to the dynamic nature of river conditions. Factors such as fluctuating discharge rates in the short term, and the potential for increased periods of low flow due to climate change in the long term, make it difficult to establish fixed timing for topping and swiping operations. In addition, unforeseen circumstances and machine availability add further complexity to the process. As a result, river dredging should be viewed as an adaptive and evolving process that requires continuous adjustment to effectively respond to changing conditions and optimise efficiency.

6 Conclusions

This study sought to enhance the comprehension of the behaviour of river dunes in the heavily dredged regions of the River Waal. A new 2D wavelet tool was developed to track and analyse river dunes. In conjunction with the dredging data, this study answered two key research questions: 1) What is the post-dredging behaviour of river dunes?

2) What is the extent of influence of the dredging method, i.e. topping or swiping, on these behaviours?

The results confirm that dredging reduces the height of river dunes and causes them to move out of their dynamic equilibrium state. After the intervention, dredged dunes, particularly topped dunes, tend to recover gradually over time, exhibiting slow development. Additionally, the study showed that larger dredging intensities yield greater growth ratios. The growth of dredged dunes exhibits less variation than that of unaffected dunes, and they appear to be more stable in the first week after dredging. This suggests that they are less susceptible to flow conditions and other fluvial processes compared to unaffected river dunes during this period.

For the dredging intensities performed in this study, topping has a more pronounced effect on the immediate reduction of dune height than swiping. The intensity of topping or swiping does not significantly affect the change in dune length. Immediately after the intervention, the dune celerity is somewhat higher for swiping. During this period, topped dunes demonstrate a more steady development pattern. Over the long term, topped dunes exhibit higher growth rates than those undergoing swiping, while the latter method is less disruptive to the sediment balance.

Acknowledgments

This study was carried out as the final component of the Civil Engineering and Management Masters degree at the University of Twente. I am extremely grateful to Lieke Lokin, Pepijn van Denderen and Suzanne Hulsscher. Their guidance and expertise have been instrumental for this work and have also enhanced my overall understanding in river morphology and the wavelet analysis. Many thanks to HKV Lijn in Water for granting me the opportunity to conduct my research within their organization. Their support and resources greatly facilitated the success of this study. Finally, I would also like to thank Ruben White (Deltares), Rolien van der Mark (Deltares) and Martijn de Graaf (Martens en Van Oord) for their insights into dune tracking and the practicalities of dredging.

References

- Allen, J. R. (1976). Relaxation time of dunes in decelerating aqueous flows. *Journal of the Geological Society*, *132*, 17 - 26. doi: 10.1144/gsjgs.132.1.0017
- Booth, A. M., Roering, J. J., & Perron, J. T. (2009). Automated landslide mapping using spectral analysis and high-resolution topographic data: Puget sound lowlands, washington, and portland hills, oregon. *Geomorphology*, *109*, 132-147. doi: 10.1016/j.geomorph.2009.02.027
- Bradley, R. W., & Venditti, J. G. (2019). The growth of dunes in rivers. *Journal of Geophysical Research: Earth Surface*, *124*, 548-566. doi: 10.1029/2018JF004835
- Bradley, R. W., & Venditti, J. G. (2021). Mechanisms of dune growth and decay in rivers. *Geophysical Research Letters*, *48*. doi: 10.1029/2021GL094572
- Brenk, van, S., Lokin, L. R., Warmink, J. J., & Hulscher, S. J. M. H. (2022). Return period of low water periods in the river rhine. In M. Ortega-Sánchez (Ed.), *Proceedings 39th iahr world congress, 19-24 june 2022, granada, spain*. IAHR. (39th IAHR World Congress 2022 : From snow to sea ; Conference date: 19-06-2022 Through 24-06-2022)
- Campmans, G. H., Roos, P. C., der Sleen, N. R. V., & Hulscher, S. J. M. H. (2021). Modeling tidal sand wave recovery after dredging: effect of different types of dredging strategies. *Coastal Engineering*, *165*. doi: 10.1016/j.coastaleng.2021.103862
- Cisneros, J., Best, J., Dijk, T. A. V., de Almeida, R. P., Amsler, M. L., Boldt, J., ... Zhang, Y. (2020). Dunes in the world's big rivers are characterized by low-angle lee-side slopes and a complex shape. *Nature Geoscience*, *13*, 156-162.

- 619 Cocard, M., Kahle, H.-G., Peter, Y., Geiger, A., Veis, G., Felekis, S., . . . Billiris,
620 H. (1999). New constraints on the rapid crustal motion of the aegean region:
621 recent results inferred from gps measurements (1993–1998) across the west
622 hellenic arc, greece. *Earth and Planetary Science Letters*, *172*(1), 39-47. doi:
623 [https://doi.org/10.1016/S0012-821X\(99\)00185-5](https://doi.org/10.1016/S0012-821X(99)00185-5)
- 624 Cox, J. R., Huismans, Y., Knaake, S. M., Leuven, J. R. F. W., Vellinga, N. E.,
625 van der Vegt, M., . . . Kleinmans, M. G. (2021). Anthropogenic effects on the
626 contemporary sediment budget of the lower rhine-meuse delta channel net-
627 work. *Earth's Future*, *9*(7), e2020EF001869. doi: [https://doi.org/10.1029/](https://doi.org/10.1029/2020EF001869)
628 [2020EF001869](https://doi.org/10.1029/2020EF001869)
- 629 Damen, J. J., van Dijk, A. T., & Hulscher, S. J. M. H. S. (2018). *Replication*
630 *data for: Spatially varying environmental properties controlling observed*
631 *sand wave morphology, part 1*. University of Twente. doi: 10.4121/uuid:
632 [0d7e016d-2182-46ea-bc19-cdfda5c20308](https://doi.org/10.4121/uuid:0d7e016d-2182-46ea-bc19-cdfda5c20308)
- 633 Denderen, van, R. P., Kater, E., Jans, L. H., & Schielen, R. M. (2022). Dis-
634 entangling changes in the river bed profile: The morphological impact
635 of river interventions in a managed river. *Geomorphology*, *408*. doi:
636 [10.1016/j.geomorph.2022.108244](https://doi.org/10.1016/j.geomorph.2022.108244)
- 637 Ding, W., Lu, C., Xie, Q., Luo, X., & Zhang, G. (2022). Understanding the settling
638 processes of dredged sediment disposed in open waters through experimental
639 tests and numerical simulations. *Journal of Marine Science and Engineering*,
640 *10*. doi: [10.3390/jmse10020220](https://doi.org/10.3390/jmse10020220)
- 641 Duffy, G. P., & Hughes-Clarke, J. E. (2005). Application of spatial cross correlation
642 to detection of migration of submarine sand dunes. *Journal of Geophysical Re-*
643 *search: Earth Surface*, *110*. doi: [10.1029/2004JF000192](https://doi.org/10.1029/2004JF000192)
- 644 Frings, R. M., & Kleinmans, M. G. (2008). Complex variations in sediment transport
645 at three large river bifurcations during discharge waves in the river rhine. *Sedi-*
646 *mentology*, *55*, 1145-1171. doi: [10.1111/j.1365-3091.2007.00940.x](https://doi.org/10.1111/j.1365-3091.2007.00940.x)
- 647 Gutierrez, R. R., Abad, J. D., Parsons, D. R., & Best, J. L. (2013). Discrimi-
648 nation of bed form scales using robust spline filters and wavelet transforms:
649 Methods and application to synthetic signals and bed forms of the río paraná,
650 argentina. *Journal of Geophysical Research: Earth Surface*, *118*, 1400-1418.
651 doi: [10.1002/jgrf.20102](https://doi.org/10.1002/jgrf.20102)
- 652 Hernandez-Hernandez, D., Larkin, T., & Chouw, N. (2021). Evaluation of the ade-
653 quacy of a spring-mass model in analyses of liquid sloshing in anchored storage
654 tanks. *Earthquake Engineering and Structural Dynamics*, *50*, 3916-3935. doi:
655 [10.1002/eqe.3539](https://doi.org/10.1002/eqe.3539)
- 656 Hulscher, S. J. M. H., & Dohmen-Janssen, C. M. (2005). Introduction to special sec-
657 tion on marine sand wave and river dune dynamics. *Journal of Geophysical Re-*
658 *search: Earth Surface*, *110*(F4). doi: <https://doi.org/10.1029/2005JF000404>
- 659 Knaapen, M. A. F., & Hulscher, S. J. M. H. (2002). Regeneration of sand waves af-
660 ter dredging. *Coastal Engineering*, *46*, 277-289. doi: [https://doi.org/10.1016/](https://doi.org/10.1016/S0378-3839(02)00090-X)
661 [S0378-3839\(02\)00090-X](https://doi.org/10.1016/S0378-3839(02)00090-X)
- 662 Laleye, K. R., Hyppolite, A., Chikou, A., Adjagbo, H., Assogba, C., Lederoun, D.,
663 & Laleye, P. (2019, 01). Inventory of estuarine and lagoonal ecosystems sub-
664 jected to sand-mining activities in southern benin (west africa). *Journal of*
665 *Environmental Protection*, *10*, 473-487. doi: [10.4236/jep.2019.104027](https://doi.org/10.4236/jep.2019.104027)
- 666 Le Coz, J., Perret, E., Camenen, B., Topping, D. J., Buscombe, D. D., Leary,
667 K. C. P., . . . Grams, P. E. (2022). Mapping 2-d bedload rates throughout
668 a sand-bed river reach from high-resolution acoustical surveys of migrat-
669 ing bedforms. *Water Resources Research*, *58*(11), e2022WR032434. doi:
670 <https://doi.org/10.1029/2022WR032434>
- 671 Lee, J. (2022). Reconstructing sediment transport by migrating bedforms in the
672 physical and spectral domains. *Water Resources Research*, *58*. doi: [10.1029/](https://doi.org/10.1029/2022WR031934)
673 [2022WR031934](https://doi.org/10.1029/2022WR031934)

- 674 Lefebvre, A. (2019). Three-dimensional flow above river bedforms: Insights
675 from numerical modeling of a natural dune field (río paraná, argentina).
676 *Journal of Geophysical Research: Earth Surface*, *124*, 2241-2264. doi:
677 10.1029/2018JF004928
- 678 Legleiter, C. J., & Kyriakidis, P. C. (2006). Forward and inverse transformations
679 between cartesian and channel-fitted coordinate systems for meandering rivers.
680 *Mathematical Geology*, *38*, 927-958. doi: 10.1007/s11004-006-9056-6
- 681 Lokin, L. R., Warmink, J. J., Bomers, A., & Hulscher, S. J. M. H. (2022). River
682 dune dynamics during low flows. *Geophysical Research Letters*, *49*. doi: 10
683 .1029/2021GL097127
- 684 Mark, van der, C. F., Blom, A., & Hulscher, S. M. J. H. (2008). Quantification of
685 variability in bedform geometry. *Journal of Geophysical Research: Earth Sur-
686 face*, *113*. doi: 10.1029/2007JF000940
- 687 Martin, R. L., & Jerolmack, D. J. (2013). Origin of hysteresis in bed form response
688 to unsteady flows. *Water Resources Research*, *49*(3), 1314-1333. doi: https://
689 doi.org/10.1002/wrcr.20093
- 690 Meijden, van der, R., Damveld, J. H., Ecclestone, D. W., der Werf, J. J. V., &
691 Roos, P. C. (2023). Shelf-wide analyses of sand wave migration using gis: A
692 case study on the netherlands continental shelf. *Geomorphology*, *424*. doi:
693 10.1016/j.geomorph.2022.108559
- 694 Mukherjee, S., Mishra, A., & Trenberth, K. E. (2018). *Climate change and drought:
695 a perspective on drought indices* (Vol. 4). Springer. doi: 10.1007/s40641-018
696 -0098-x
- 697 Naqshband, S., Hurther, D., Giri, S., Bradley, R. W., Kostaschuk, R. A., Venditti,
698 J. G., & Hoitink, A. J. F. (2021). The influence of slipface angle on flu-
699 vial dune growth. *Journal of Geophysical Research: Earth Surface*, *126*(4),
700 e2020JF005959. doi: https://doi.org/10.1029/2020JF005959
- 701 Patmont, C. (2018). Environmental dredging residual generation and management.
702 *Integrated Environmental Assessment and Management*, *14*. doi: 10.1002/ieam
703 .4032
- 704 Reesink, A. (2018). The adaptation of dunes to changes in river flow. *Earth-Science
705 Reviews*. doi: 10.1016/J.EARSCIREV.2018.09.002
- 706 Ruijsscher, de, T. V., Naqshband, S., & Hoitink, A. J. (2020). Effect of non-
707 migrating bars on dune dynamics in a lowland river. *Earth Surface Processes
708 and Landforms*, *45*, 1361-1375. doi: 10.1002/esp.4807
- 709 Savitzky, A., & E, M. J. (1951). *Smoothing and differentiation of data by simplified
710 least squares procedures* (Vol. 40).
- 711 Struble, W. T., Roering, J. J., Dorsey, R. J., & Bendick, R. (2021). *Characteris-
712 tic scales of drainage reorganization in cascadia* (Vol. 48). Blackwell Publishing
713 Ltd. doi: 10.1029/2020GL091413
- 714 Torrence, C., & Compo, G. P. (1998). A practical guide to wavelet analysis. *Ameri-
715 can Meteorological Society*, *79*, 61-78. doi: 10.1175/1520-0477(1998)079%
716 3C0061:APGTWA%3E2.0.CO;2
- 717 Warmink, J. J. (2014). Dune dynamics and roughness under gradually varying flood
718 waves, comparing flume and field observations. *Advances in Geosciences*, *39*,
719 115-121. doi: 10.5194/adgeo-39-115-2014
- 720 Zomer, J. Y., Naqshband, S., & Hoitink, A. J. (2022). Short communication: A tool
721 for determining multiscale bedform characteristics from bed elevation data.
722 *Earth Surface Dynamics*, *10*, 865-874. doi: 10.5194/esurf-10-865-2022
- 723 Zomer, J. Y., Naqshband, S., Vermeulen, B., & Hoitink, A. J. (2021). Rapidly
724 migrating secondary bedforms can persist on the lee of slowly migrating pri-
725 mary river dunes. *Journal of Geophysical Research: Earth Surface*, *126*. doi:
726 10.1029/2020JF005918